nature communications

Article

https://doi.org/10.1038/s41467-025-57984-3

Temporal stability of forest productivity declines over stand age at multiple spatial scales

Received: 21 May 2024

Accepted: 10 March 2025

Published online: 20 March 2025

Check for updates

Rongxu Shan[1], Ganxin Feng[1], Yuwei Lin[2,3] & Zilong Ma[1]

There is compelling experimental evidence and theoretical predictions that temporal stability of productivity, i.e., the summation of aboveground biomass growth of surviving and recruitment trees, increases with succession. However, the temporal change in productivity stability in natural forests, which may undergo functional diversity loss during canopy transition, remains unclear. Here, we use the forest inventory dataset across the eastern United States to explore how the temporal stability of forest productivity at multi-spatial scales changes with stand age during canopy transition. We find that productivity stability decreases with stand age at the local and metacommunity scales. Specifically, consistent declines in local diversity result in less asynchronous productivity dynamics among species over succession, consequently weakening local stability. Meanwhile, increasing mortality and the transition from conservative to acquisitive species with succession weaken species and local stability. Successional increases in species composition dissimilarity among local communities cause more asynchronous productivity dynamics among local communities. However, the decline in local stability surpasses the rise in asynchronous productivity dynamics among local communities, resulting in lower metacommunity stability in old forests. Our results suggest lower productivity stability in old-growth forests and highlight the urgency of protecting diversity at multiple spatial scales to maintain productivity stability.

Temporal stability of forest aboveground productivity (i.e., the ratio of mean productivity, which is the summation of aboveground biomass growth of surviving trees and in-growth by new recruitment trees, to its variation in time) is a widely accepted measure of forests' ability to maintain productivity over time[1,2]. Traditional succession studies have focused on the community states, such as biomass and cover, with recent field experiments showing that their temporal stability increases with succession at multiple spatial scales[3,4]. However, how the temporal stability of productivity changes during late-successional stages in natural forests remains unclear at multiple spatial scales. Elucidating these dynamics will help managers ensure the stable provisioning of ecosystem services and efficient restoration practices under future conditions[5–7].

Recently, a multiscale stability framework has shown that temporal stability at the larger scale (i.e., metacommunity stability) can be decomposed into temporal stability at the smaller scale (i.e., local stability) and spatial asynchrony, i.e., asynchronous productivity dynamics among local communities under heterogenous spatial environments[8–10]. Similarly, local stability can be decomposed into species stability and species asynchrony, i.e., temporal stability of

[1]School of Ecology, Shenzhen Campus of Sun Yat-sen University, Guangdong 518107, China. [2]Shapotou Desert Research and Experiment Station, Northwest Institute of Eco-environment and Resource Research, Chinese Academy of Sciences, Lanzhou, China. [3]University of Chinese Academy of Sciences, Beijing, China. e-mail: mazlong@mail.sysu.edu.cn

productivity at the population level and asynchronous population dynamics in local communities. The multiscale stability framework can capture the scale dependence of ecosystem temporal stability over succession, i.e., higher stability at larger scales because deterministic processes (e.g., environmental filtering) dominate community assembly at the metacommunity scale whereas stochastic processes (e.g., random dispersal) dominate at the local scale[3,11–13]. However, change in temporal stability over stand age at multiple spatial scales has received little attention, particularly in late successional stages dominated by conservative species, due to the lack of long-term and nested permanent plot measurements of forest dynamics.

Increasing local species diversity and species composition dissimilarity among local communities with stand age contributes to the successional increase in metacommunity stability during early field succession experiments[3,4]. On the one hand, increasing canopy complexity with succession strengthens competition for light resources[14,15], which promotes the coexistence of conservative species with high shade tolerance and acquisitive species with an efficient ability to utilize canopy light resources, resulting in higher local diversity[16–19]. Local stability tends to increase with local diversity because differentiated species functional strategies enable local communities to exhibit higher species asynchrony, i.e., the productivity gain of suitable species compensates for the productivity loss of unsuitable species (compensatory effects)[1,18,20,21]. On the other hand, as stands develop, stochastic processes (e.g., dispersal limitation and colonization) prompt divergent trajectories over succession among local communities[22–25]. Meanwhile, initial habitat heterogeneity among local communities could facilitate or inhibit the colonization of different species, resulting in higher species composition dissimilarity among local communities[24,26]. Dissimilarity among local communities stabilizes forest productivity against spatial environmental heterogeneity from the neighborhood scale (tens of meters) to the landscape scale (tens of kilometers), resulting in higher spatial asynchrony[12,27,28]. However, increasing local diversity and dissimilarity among local communities during forest succession is not always expected, especially not until late successional stages, which leads to uncertainty about the temporal stability of old forests.

Decreasing local diversity and increasing dissimilarity among local communities make predicting changes in metacommunity stability during later forest succession difficult. As stands enter the canopy transition stage, overstory acquisitive species approach their lifespan and release canopy space after mortality, while understory conservative species with asymmetric competitive advantages occupy the forest canopy[17,29,30]. Although acquisitive species may experience increased recruitment in the understory due to their abundant seeds, their shade intolerance makes it difficult for them to occupy the canopy under the asymmetric advantage of conservative species when stand-replacing disturbances are infrequent[17,31,32]. This successional trajectory results in the transition from the coexistence of conservative species and acquisitive species to the dominance of conservative species, resulting in lower local diversity[32–36]. This diversity loss will lead to lower species asynchrony and temporal stability in local communities[1,20]. Meanwhile, stochastic mortality of overstory acquisitive species will allow conservative species to dominate the newly opened gap when stand-replacing disturbances are infrequent, resulting in higher species composition dissimilarity among local communities which leads to spatial asynchrony[12,29,37]. Previous studies have shown that increasing local stability or spatial asynchrony can both independently cause successional increases in temporal stability[3,4]. However, whether reduced local stability or increased spatial asynchrony contributes more to metacommunity stability is unclear.

In this work, we used the national forest survey dataset from the eastern United States to explore how stand age changes temporal stability in natural forests at multiple spatial scales (Supplementary Fig. 1). This dataset is well-suited for studying multiscale stability because each plot in the FIA program contains four circular subplots: one in the center and the other three arranged in a triangular pattern around it (Supplementary Fig. 2). We considered each subplot as a local community and each plot, comprising four subplots, as a metacommunity. Given that functional strategies can effectively capture plant responses to climate change, we used functional diversity to explore how changing diversity alters temporal stability with stand age[3,38]. Specifically, we examined 1) whether older forests exhibit higher temporal stability at the metacommunity and local scales (Fig. 1); and 2) whether this pattern is attributed to changes in local functional diversity and functional dissimilarity among local communities over stand age. We show decreasing diversity with forest age reduces temporal stability at multiple spatial scales, suggesting the urgency of protecting old-growth forests to ensure forest ecosystem services provisioning under climate change threats.

Results

Stand age weakens temporal stability at multiple scales

We found that temporal stability of productivity at both the metacommunity scale and the local community scale decreased with stand age, but spatial asynchrony did not show a significant relationship with stand age (Fig. 2, estimate [±SE] = −0.370 [0.020], $t_{2875} = -15.538$, $P < 0.001$ for local stability, estimate [±SE] = −0.582 [0.037], $t_{2875} = -15.538$, $P < 0.001$ for metacommunity stability and estimate [±SE] = 0.004 [0.007], $t_{2843} = 0.508$, $P = 0.612$ for spatial asynchrony). After decomposing local stability into species stability and species asynchrony, our results showed that both species stability and species asynchrony decreased with stand age (Fig. 1, estimate [±SE] = −0.258 [0.015], $t_{2860} = -17.655$, $P < 0.001$ for species stability and estimate [±SE] = −0.022 [0.004], $t_{2878} = -5.822$, $P < 0.001$ for species asynchrony). Besides spatial asynchrony, stand age was the major driver for stability at multiple scales (Supplementary Fig. 3A and Supplementary Table 1). Similar results were found in our sensitivity analysis which considered detrended stability (Supplementary Fig. 4), different ecoregions (Supplementary Fig. 5), other confounding variables (Supplementary Fig. 6A and Supplementary Fig. 7; observational frequency, survey interval, initial survey year, and final survey year), stand structure (Supplementary Fig. 8), and biomass loss due to mortality (Supplementary Fig. 8). Decreasing mean productivity and increasing standard deviation of productivity with stand age jointly contributed to successional declines in temporal stability (Supplementary Fig. 9 and Supplementary Fig. 10).

Stand age reduce diversity at multiple scales

Functional diversity at both the metacommunity scale and the local community scale decreased with stand age, but functional dissimilarity among local communities increased with stand age (Fig. 3, estimate [±SE] = −0.025 [0.007], $t_{2877} = -3.423$, $P < 0.001$ for local functional diversity, estimate [±SE] = 0.039 [0.015], $t_{2877} = 2.613$, $P = 0.009$ for functional dissimilarity among local communities, and estimate [±SE] = −0.020 [0.009], $t_{2876} = -2.210$, $P = 0.027$ for metacommunity functional diversity). After considering confounding factors (observational frequency, survey interval, initial survey year, and final survey year), the trends of functional diversity with stand age at multiple spatial scales remained unchanged (Supplementary Figs. 3B, Supplementary Fig. 6B, and Supplementary Table S2). Similar results were found using the Shannon diversity index, but there was a non-significant relationship between metacommunity diversity and stand age (Fig. 3, estimate [±SE] = −0.018 [0.005], $t_{2878} = -3.364$, $P < 0.001$ for local Shannon diversity, estimate [±SE] = 0.063 [0.002], $t_{2874} = 3.656$, $P < 0.001$ for composition dissimilarity among local communities, and estimate [±SE] = −0.008 [0.008], $t_{2803} = -1.042$, $P = 0.297$ for metacommunity Shannon diversity).

https://doi.org/10.1038/s41467-025-57984-3

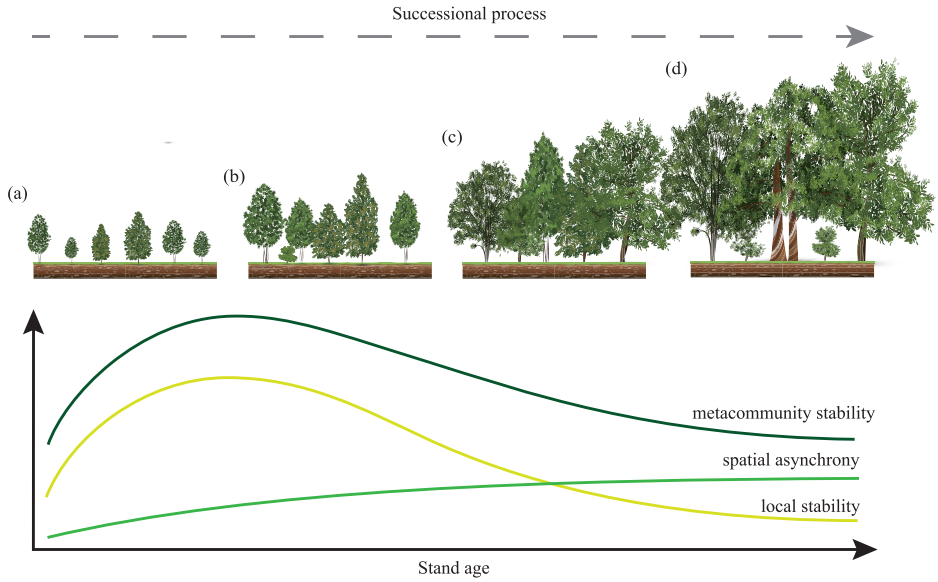

Fig. 1 | A conceptual diagram showing four stages of forest succession and expected changes in temporal stability with succession. a stand establishment: After suffering disturbances like fire, high resource availability promotes the colonization of fast-growing species, usually *Pinus* in eastern US forests; (**b**) stem exclusion: competition for light and canopy space intensifies, and conservative species grow understory; (**c**) canopy transition: overstory fast-growing species die due to lifespan limitation, and shade-tolerant conservative species occupy canopy, usually *Abies* and *Quercus* in eastern US forests; (**d**) gap dynamics: conservative species dominate forest canopy, usually *Quercus* and *Carya*, and shade-intolerant trees occupied gaps. Our results about species composition over stand age show that most plots are in the canopy transition stage (Fig S20) because late-successional species (*Quercus* and *Acer*) are replacing the pioneer species (*Pinus* and *Liquidambar*). Tree images in Fig. 1 were designed by macrovector - Freepik.com.

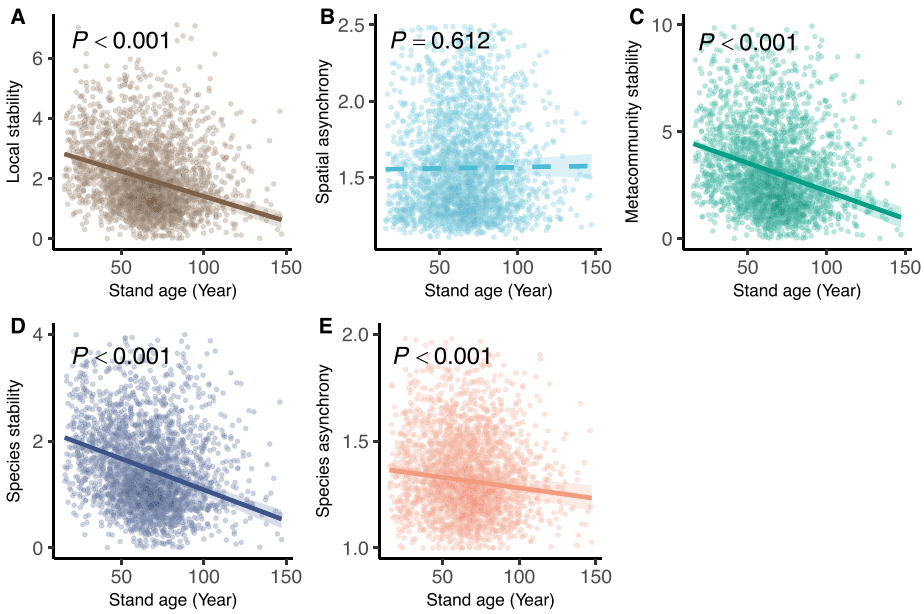

Fig. 2 | Trends associated with stand age and five temporal stability components. A local stability, **B** spatial asynchrony, **C** metacommunity stability, **D** species stability, and **E** species asynchrony. Dots are the values predicted by partial regressions with each explanatory variable. The lines and shades are the mean and 95% confidence intervals. Source data are provided as a Source Data file.

Decreasing diversity with stand age reduces temporal stability

We found significant diversity-stability relationships at both local and metacommunity scales (Fig. 4 and Supplementary Fig. 11). Specifically, functional and local Shannon diversity were both positively associated with local stability at the local scale (Figs. 4A and Supplementary Fig. 11A, estimate [±SE] = 0.253 [0.055], $t_{2844} = 4.570$, $P < 0.001$ for local functional and estimate [±SE] = 0.287 [0.077], $t_{2833} = 3.726$, $P < 0.001$ for Shannon diversity); functional and composition dissimilarity among local communities were both positively associated with spatial asynchrony (Fig. 4D and Supplementary Fig. 11D, estimate [±SE] = 0.030 [0.009], $t_{2757} = 3.448$, $P < 0.001$ for functional dissimilarity among local communities and estimate [±SE] = 0.025 [0.007], $t_{2524} = 3.391$, $P < 0.001$ for composition dissimilarity among local communities); metacommunity functional diversity was positively associated with metacommunity stability at the metacommunity scale, but there was no significant relationship between metacommunity Shannon diversity and metacommunity stability (Fig. 4E and Supplementary Fig. 11E, estimate [±SE] = 0.185 [0.081], $t_{2884} = 2.259$, $P = 0.024$

https://doi.org/10.1038/s41467-025-57984-3

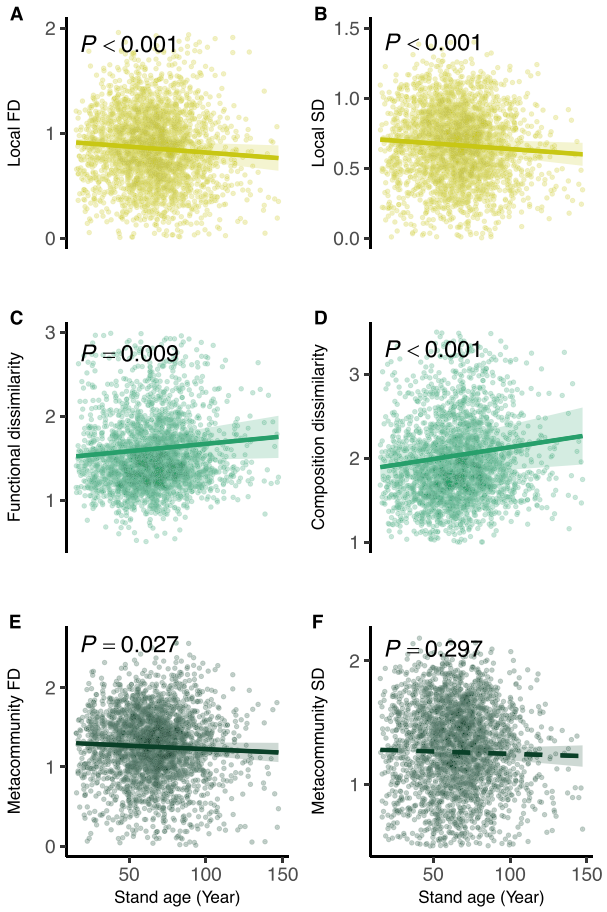

Fig. 3 | Trends associated with stand age and six diversity components. A local functional diversity, **B** local Shannon diversity, **C** functional dissimilarity among local communities, **D** composition dissimilarity among local communities, **E** metacommunity functional diversity, and **F** metacommunity Shannon diversity). FD functional diversity. Two-sided t test was used to test whether there is a significant difference in slope from 0. Dots are the values predicted by partial regressions with each explanatory variable. The lines and shades are the mean and 95% confidence intervals. Source data are provided as a Source Data file.

for metacommunity functional diversity and estimate [±SE] = −0.078 [0.089], $t_{2883} = -0.877$, $P = 0.381$ for metacommunity Shannon diversity). Meanwhile, both local functional and Shannon diversity increased species asynchrony (estimate [±SE] = 0.252 [0.008], $t_{2702} = 30.210$, $P < 0.001$ for local functional and estimate [±SE] = 0.433 [0.012], $t_{2669} = 40.910$, $P < 0.001$ for Shannon diversity) but decreased species stability at the local scale (Fig. 4 and Supplementary Fig. 11; estimate [±SE] = −0.130 [0.039], $t_{2844} = -3.309$, $P < 0.001$ for local functional and estimate [±SE] = −0.314 [0.055], $t_{2883} = -5.753$, $P < 0.001$ for Shannon diversity). Similar results were found when considering changes in functional diversity during the survey (Supplementary Fig. 12) and using the functional dissimilarity among local communities considering effective species number (Supplementary Fig. 13).

Our SEM showed that decreasing local functional diversity with stand age significantly reduced metacommunity stability by weakening local stability. Further, increasing functional dissimilarity among local communities with stand age significantly enhanced metacommunity stability at the metacommunity scale by promoting spatial asynchrony (Fig. 5A and Supplementary Fig. 14A). Decreasing local functional diversity with stand age weakened species asynchrony, and stand age directly decreased species stability, leading to decreasing local stability with stand age (FigS. 5B and Supplementary Fig. 14B). Consequently, local functional diversity exhibited stronger stabilizing effects on local stability than functional dissimilarity among local communities on spatial asynchrony, resulting in decreasing metacommunity stability with stand age. After aggregating each plot and its three nearest plots into one community at the larger scale, decreasing metacommunity stability exceeds the stabilizing effects of spatial asynchrony from the metacommunity to the larger scale, resulting in decreasing stability at the larger scale with stand age (Supplementary Fig. 15). Structural equation modeling based on the Shannon diversity index produced similar results (Supplementary Fig. 16 and Supplementary Fig. 17). Meanwhile, increased CWM_{PC1} with stand age weakened species stability but strengthened species asynchrony; lower CWM_{PC2} as stands aged weakened species asynchrony but had no effect on species stability (Supplementary Fig. 18). Increased mortality as stands aged weakened species stability and local stability (Supplementary Fig. 19).

Discussion

Our study of forest communities across broad stand age gradients reveals weakened temporal stability during late forest succession at multiple spatial scales. Specifically, we found a clear pattern that local stability decreased but spatial asynchrony marginally increased with stand age, coupled with stronger stabilizing effects of local stability than spatial asynchrony on metacommunity stability, which prompted older forests to exhibit lower temporal stability of productivity at the metacommunity scale.

As hypothesized, local functional diversity decreased as stands aged during the later stages of forest succession. Successional theory typically predicts the highest diversity during mid-successional stages in temperate forests, as conservative species with high shade tolerance and pioneer species with high resource acquisition ability simultaneously occupy their respective ecological niches[17,34,35,39]. As stands enter the canopy transition stage, mortality of overstory pioneer species disrupts this balance. Released light resources and canopy space from this mortality favor shade-tolerant species in the understory, as they have accumulated asymmetric competitive advantages under shade conditions during the stem exclusion stage[17,30,40]. Low recruitment of pioneer species under low light availability cannot compensate for their mortality, resulting in shade-tolerant species dominance and lower diversity in old-growth forests compared to mid-successional forests[32–34].

Diversity loss with stand age causes old-growth forests to exhibit low local stability. This negative relationship between functional diversity and species stability hasn't been observed in previous tree-planting experiments[1]. The discrepancy may arise because increased functional diversity intensifies heterospecific competition and reduces the species stability of the dominant species, but the short duration of planting experiments limits canopy competition[20,41–44]. Asynchronous population dynamics compensate for this decreasing species stability, resulting in higher local stability in more diverse communities[20]. Therefore, diversity loss over stand age results in lower species asynchrony and local stability under climate change. Moreover, the shift from coniferous to broad-leaved species in eastern United States forests (Supplementary Fig. 20) facilitates the transition from conservative to acquisitive species over succession, as broad-leaved species typically exhibit higher specific leaf area and leaf nitrogen content than coniferous species[45]. This transition weakens species stability, as acquisitive and broad-leaved species typically exhibit weaker tolerance to environmental stress than conservative and coniferous species[45,46]. The shift from stress-intolerant to tolerant species with succession reduces species asynchrony, as high wood density increases construction costs and reduces trait plasticity, which weakens compensatory effects under climate change[47,48].

Stand age may also directly weaken species stability through changes in resource allocation during individual development. Trees typically allocate more resources for growth before reaching the

https://doi.org/10.1038/s41467-025-57984-3

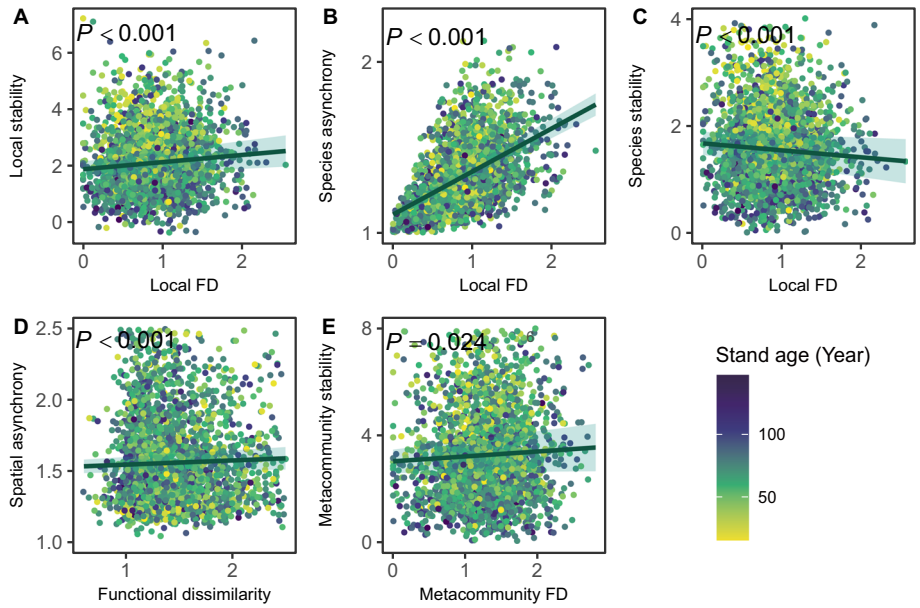

Fig. 4 | Trends associated with functional diversity-stability relationships with color gradient showing stand age. A local stability, **B** spatial asynchrony, **C** metacommunity stability, **D** species stability, and **E** species asynchrony. FD functional diversity. Two-sided t test was used to test whether there is a significant difference in slope from 0. Dots are the values predicted by partial regressions with each explanatory variable. The lines and shades are the mean and 95% confidence intervals. Source data are provided as a Source Data file.

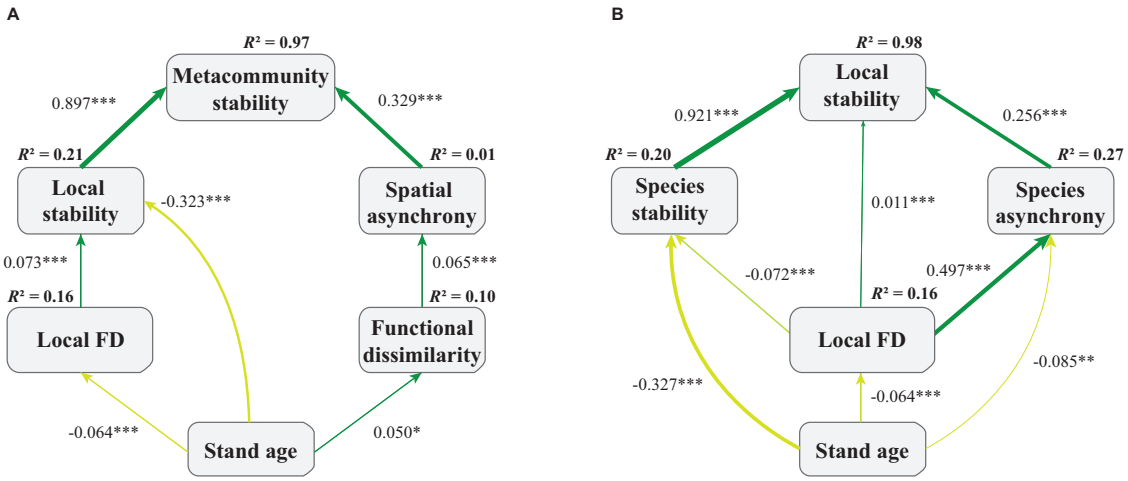

Fig. 5 | The structural equation modelings showing the changes of temporal stability over succession across spatial scales and how they relate to biodiversity. The structural equation modeling shows how changes in functional diversity with stand age regulate (**A**) metacommunity and (**B**) local stability. The green and yellow arrows show positive and negative significant paths with standardized coefficients shown (*: $P < 0.05$, **: $P < 0.01$, and ***: $P < 0.001$). Conditional R^2 is shown in corresponding boxes. Two-sided Fisher's C test was used to test whether significant paths had not been included in the models. The SEMS fit the data well (**A**) Fisher's C = 29.319, df = 42, $P = 0.93$; **B** Fisher's C = 18.855, df = 18, $P = 0.401$). The full SEMs with all paths are shown in the supplementary materials (Supplementary Fig. 10). Source data are provided as a Source Data file.

canopy but shift those resources toward defense and respiration during late ontogeny; older trees exhibit higher metabolism costs to maintain complex tissue structures and convert sapwood towards heartwood[49–51]. Meanwhile, longer water transport paths and stronger hydrostatic stress also increase the hydraulic costs of old trees[52,53]. This resource allocation pattern causes a strong sensitivity of older trees to climate change, especially water availability, leading to declining species stability as stands age[54,55]. Meanwhile, increasing mortality with stand age releases canopy space and promotes the growth of neighboring trees, but this stochastic tree mortality also increases variation in individual productivity, resulting in lower species stability[30,56].

As we hypothesized, functional dissimilarity among local communities increased with stand age, resulting in stronger spatial asynchrony. Previous studies have shown that dissimilarity among local communities increases with succession due to stronger stochastic processes in community assembly mechanisms[3,11,22]. Specifically, older forests exhibit stronger spatially stochastic mortality patterns due to density-independent mortality of canopy pioneer trees, resulting in spatial stochasticity of canopy transitions from acquisitive species to conservative species[17,29,30,57]. Meanwhile, environmental filtering due to stochastic climatic events and dispersal limitations drive more dissimilar species composition among local communities, leading to higher functional dissimilarity among local communities[11,24,58]. Our

results also support that functional dissimilarity among local communities contributes to asynchronous productivity dynamics under spatial environmental heterogeneity, resulting in stronger metacommunity stability[3,12,27,59].

Our study shows that although local stability and spatial asynchrony both promote metacommunity stability, increasing spatial asynchrony can not compensate for the decreasing local stability as stands age, which results in lower metacommunity stability in old-growth forests. We highlight the importance of preserving local diversity during succession to maintain multiscale temporal stability of productivity[4,21,28]. Our observation of a decline in species diversity during canopy transition is inconsistent with the increasing diversity and stability observed with succession in previous studies[3,4,36]. Even the 60-year old abandoned field experiment is still in the early stages of forest succession, where pioneer species dominate (e.g., *Juniperus virginiana*), making it difficult to detect the local diversity loss due to the canopy transition from pioneer to shade-tolerant species[3,11]. Weaker stabilizing effects of dissimilarity among local communities on spatial asynchrony and metacommunity stability may result from small spatial ranges and low environmental heterogeneity[28,60]. Recent studies have also shown that greater environmental heterogeneity caused by larger spatial ranges enhances the stabilizing effect of dissimilarity among local communities[27,59].

While the FIA dataset provides an opportunity to assess successional changes in temporal stability across multiple spatial scales, there are several caveats worth noting. First, the space-for-time approach we utilized is often criticized for potentially overlooking diverse successional trajectories across varied environments[61,62]. To mitigate this concern, we conducted separate analyzes for ecoregions characterized by similar environmental conditions and potential communities, which consistently supported our conclusions (Supplementary Fig. S5). Second, our analysis did not address environmental heterogeneity among subplots, which could influence the role of environmental filtering in spatial asynchrony[9]. Third, temporal stability is often recommended to be calculated with relatively high temporal resolution, while the fixed census interval of the FIA dataset is approximately five years. Although our results show that productivity fluctuations with a five-year interval contribute to the declining temporal stability over stand age (Supplementary Fig. 9), future research utilizing shorter intervals, such as two or three years, would be valuable for better generalizing our observed patterns. Fourth, while we demonstrated that temporal stability decreases with forest age across local and metacommunity scales (Fig. 5 and Supplementary Fig. 15), future research could incorporate composite plots of varying sizes to more effectively capture the dynamics of woody species such as tree mortality.

In conclusion, our findings provide rare evidence for the diversity-stability relationship at multiple spatial scales in natural forests[2], and extend stability studies from field succession experiments to late successional stages in natural forests[3,4]. Specifically, we find that after stands enter the canopy transition stage, local diversity loss due to community composition towards shade-tolerant species decreases temporal stability of productivity at multiple spatial scales. Our results indicate that the decreasing local stability caused by local diversity loss will extend to the metacommunity and landscape scales, highlighting the need to restore biodiversity at multiple spatial scales to maintain ecosystem stability[63]. We also suggest the urgency of protecting old-growth forests to ensure forest ecosystem services provisioning under climate change threats[64,65].

Methods

Study area and forest inventory data

We accessed the dataset from the United States Department of Agriculture's Forest Inventory and Analysis (FIA) program (available at https://www.fia.fs.usda.gov/tools-data/). The FIA program used a network of permanent plots to observe spatial and temporal patterns of forest resources across the United States, with a sampling intensity of approximately one plot every 2428 ha. Each plot contains four circular subplots of a 7.32 m radius, with one subplot located in the center and the other three subplots 36.6 m apart from the central subplot in a triangular arrangement (Supplementary Fig. 2). The national hierarchical framework of ecological units assigned each plot to an ecoregion with similar climatic regime and topography, and potentially similar forest type and other abiotic factors (e.g., soil and physiography)[66]. Within each plot, diameter at breast height (DBH) and species identity were recorded periodically between 1995 and 2022 for all stems with DBH > 12.7 cm. FIA calculated the individual aboveground volume based on species and region-specific DBH-volume equations and then calculated the aboveground biomass based on species-specific density information[67]. The stand age at the plot level was estimated by counting growth rings on increment cores taken from two or three dominant or codominant trees in the stand-size class (three stand-size classes with minimum DBH values of 0 cm, 12.7 cm, and 22.9 cm) with the highest canopy cover. If the overstory contained a wide range of tree species, field crews tried to select the trees accordingly and calculated the weighted average stand age based on canopy cover.

We used the following screening criteria: 1) plots followed standardized production and survey methods; 2) plots were distributed in natural forests with no artificial (e.g., silvicultural treatments and selective logging) or natural disturbances (e.g., fire and insect outbreaks) recorded; 3) trees were present in all four subplots; 4) species names were recorded for all trees in the plot; 5) there were at least four measurements (i.e., at least three productivity measurements) with stand age recorded to calculate temporal stability. This left us with 2, 866 plots (Fig. S21, stand age: 65.6 ± 22.3 years, mean ± s.d.) with 89, 309 trees and 134 tree species (Fig. S1; 25.85°N-48.86°N, 67.13°W-96.30°W). All plots were situated in the eastern region of the United States, as longer survey intervals and more frequent natural and artificial disturbances removed plots in the western region. Among the 2886 plots included in the study, 1893 were measured four times, 940 were measured five times, and 53 were measured six times. The observational period ranged from 11 to 24 years (17.0 ± 2.6 years). The observational interval was 5.05 ± 1.36 years. Mean annual temperatures (MAT) ranged from 3.2 °C to 24.1 °C and mean annual precipitation (MAP) ranged from 51.4 to 150.7 cm.

Temporal stability components

Biomass productivity was calculated as the biomass growth of surviving trees and in-growth by new recruitment trees between two consecutive censuses divided by interval time. We regarded each subplot as a local community and each plot containing four subplots as a metacommunity. Following the multiscale stability theory[8–10], temporal stability at the metacommunity scale is equal to the temporal stability at the local scale times the spatial asynchrony among local communities.

$$\text{local stability} = \frac{\sum_{i,k}\mu_{i,k}}{\sum_{k}\sqrt{\sum_{i,j}v_{ij,kk}}} \tag{1}$$

$$\text{spatial asynchrony} = \frac{\sum_{k}\sqrt{\sum_{i,j}v_{ij,kk}}}{\sqrt{\sum_{i,j,k,l}v_{ij,k,l}}} \tag{2}$$

$$\begin{aligned}\text{metacommunity stability} &= \text{local stability} \times \text{spatial asynchrony}\\ &= \frac{\sum_{i,k}\mu_{i,k}}{\sqrt{\sum_{i,j,k,l}v_{ij,k,l}}}\end{aligned} \tag{3}$$

where i, j, k, l mean species i and j, and local community k and l, respectively. $\mu_{i,k}$ means the mean productivity of species i in the local community k during the survey; $\sum_{i,k}\mu_{i,k}$ means the summing average productivity of all species in four local communities in a metacommunity; $v_{ij,kk}$ means the productivity covariance between species i and species j in local community k during the survey; $\sum_{i,j}v_{ij,kk}$ means the summing productivity covariance between all species pairs in a local community k; $v_{ij,k,l}$ means the productivity covariance between species i in local community k and species j in local community l during the survey. $\sum_{i,j,k,l}v_{ij,k,l}$ means the summing productivity covariance between all species pairs in a metacommunity. Local stability measures the degree of productivity fluctuations over time at the local community scale. It is always greater than 0, with higher values indicating less fluctuation and greater stability. Metacommunity stability assesses productivity fluctuations over time at the metacommunity scale. It is greater than 0, with larger values signifying less fluctuation and more stability. Spatial asynchrony refers to the variability in productivity among different local communities within one metacommunity. This value is greater than or equal to 1, with a value of 1 indicating consistent changes in productivity across all local communities, while larger values signify more inconsistent changes. Similarly, local stability equals species stability times species asynchrony.

$$\text{species stability} = \frac{\sum_{i,k}\mu_{i,k}}{\sum_{i,k}\sqrt{v_{ii,kk}}} \tag{4}$$

$$\text{species asynchrony} = \frac{\sum_{i,k}\sqrt{v_{ii,kk}}}{\sum_{k}\sqrt{\sum_{i,j}v_{ij,kk}}} \tag{5}$$

where $\mu_{i,k}$ means the mean productivity of species i in the local community k during the survey; $v_{ii,kk}$ means the productivity variance of species i in the local community k during the survey. $\sum_{i,k}\sqrt{v_{ii,kk}}$ means the summing productivity standard deviation of all species in local community k. Species stability denotes the fluctuational degree of productivity over time for all species within one local community. It is always greater than 0, with higher values indicating less fluctuation and greater stability. Species asynchrony denotes the variability in productivity over time among different species within one local community. This value is greater than or equal to 1, where 1 represents a consistent change in productivity over time across all species, and larger values indicate more inconsistency.

Functional traits

We selected five functional traits, which were considered to reflect tree resource acquisition strategy and how trees respond to climate change[46,48], including specific leaf area (SLA, $mm^2\ mg^{-1}$), leaf dry matter content (LDMC, $mg\ g^{-1}$), wood density (WD, $g\ m^{-3}$), nitrogen content per leaf mass (N_{mass}, $mg\ g^{-1}$) and phosphorus content per leaf mass (P_{mass}, $mg\ g^{-1}$). We obtained species mean trait values from the TRY database[68] and then replaced missing trait values with genus-level means, but 1.5%-11.9% of trait values were still missing. We constructed the phylogenetic tree for the 134 species in our dataset and obtained the phylogenetic distance matrix based on the '*V.PhyloMaker*' package[69]. We used the random forest algorithm containing the first 10 eigenvectors calculated from the phylogenetic distance matrix to impute the remaining missing trait values based on the '*Missforest*' package[70]. We calculated the community-weighted trait means (CWM), using the relative basal area as the weighting factor to reflect functional strategies at the plot level[1]. Subsequently, we performed a principal component analysis (PCA) based on the CWMs of five traits (Supplementary Fig. 22A). CWM_{PC1}, which explained 56.7% of the variation, was positively correlated with CWM_{SLA}, CWM_{Nmass}, and CWM_{Pmass}, and negatively correlated with CWM_{LDMC}, indicating traits associated with acquisitive growth strategies; CWM_{PC2}, which accounted for 20.4% of the variation, was negatively correlated with CWM_{WD}, reflecting stress intolerant strategies.

Quantification of biodiversity and environmental drivers

We calculated functional dispersion, i.e., the mean distance of each species to the abundance-weighted centroid of all species in a functional multidimensional space, as the measure of functional diversity[71]. Specifically, local functional diversity was measured as mean functional dispersion based on the above five functional traits in local subplots across all observation years. Metacommunity functional diversity was measured as mean functional dispersion at the metacommunity across all observation years. Functional dissimilarity among local communities was defined as the ratio of metacommunity functional diversity to local functional diversity[8,9]. Similarly, we also calculated the Shannon diversity index to strengthen the robustness of our results.

To control the influence of the regional environment on stability, we extracted the following environmental variables as covariates to study the trend of stability with stand age. Monthly mean temperature, potential evapotranspiration, and precipitation between 1997 and 2022 were derived from a gridded multivariate climate dataset with a resolution of 0.5° × 0.5°[72]. We then calculated the long-term average of climate moisture index (CMI) and mean annual temperature (MAT) between 1997 and 2022. CMI was equivalent to annual precipitation minus annual potential evapotranspiration and represented climate water availability. To measure the interannual fluctuations of climate during the survey, we also calculated the coefficients of variation of the annual mean temperature (CVT) and climate moisture index (CVM). Additionally, plot-level information on key soil properties [pH in H_2O (pH), organic carbon content ($g\ kg^{-1}$, SOC), total nitrogen ($g\ kg^{-1}$, TOTN), cation exchange capacity ($cmol\ kg^{-1}$, CEC) of the 0-30 cm soil horizon] was obtained from SoilGrids[73]. A principal component analysis was performed using these four soil properties to assess overall soil conditions (Supplementary Fig. 22B). The first principal component ($Soil_{PC1}$), which explained 69.9% of the variation and showed positive associations with TOTN, SOC, and CEC, and the second principal component ($Soil_{PC2}$), explaining 18.2% of the variation and negatively associated with pH, were ultimately selected.

Statistical analyzes

To explore how five temporal stability components (metacommunity stability, local stability, spatial asynchrony, species stability, and species asynchrony) and three diversity components (local and metacommunity functional diversity, and functional dissimilarity among local communities) change with stand age, we fitted the following linear mixed effects model using the '*lme4*' package with restricted maximum likelihood estimation[74]:

$$\begin{aligned}\text{Stability}_i/\text{Diversity}_i = {} & \beta_1 \times SA_i + \beta_2 \times MAT_i + \beta_3 \times CMI_i + \beta_4 \times Soil_{PC1i} \\ & + \beta_5 \times Soil_{PC2i} + \beta_6 \times CVT_i + \beta_7 \times CVM_i + \pi_i + \varepsilon\end{aligned} \tag{6}$$

where i is ith plot; β is the estimated coefficients in the model; Stability_i means five temporal stability components in ith plot; Diversity_i means three diversity components in ith plot; SA_i is the mean stand age of all observed years in ith plot; MAT_i, CMI_i, CVT_i, and CVM_i are mean annual temperature, climate moisture index, and the coefficients of variation of the annual mean temperature and climate moisture index in ith plot, respectively; $Soil_{PC1}$ and $Soil_{PC2}$ are the soil properties in two axes based on PCA (Supplementary Fig. 22B). π_i is a random ecoregion effect accounting for site-specific regional climate and geology; ε is a random error. Considering the potential non-linear relationship between stability and stand age, we performed logarithmic and quadratic transformations on stand age based on Akaike Information Criteria (AIC; Supplementary Table S3). All transformations indicated

that multiscale stability decreased with succession (Supplementary Fig. 23). To maintain the accuracy of the original data, we report the results without transformation in the main text. All predictor variables were scaled to facilitate coefficient comparison. Similarly, we also fitted univariate linear mixed models to test how functional diversity affects ecosystem stability at multiple spatial scales.

To explore direct and indirect drivers of variation in metacommunity stability with stand age, we fitted the piecewise structural equation modeling using the '*piecewiseSEM*' package based on the priori theoretical framework (Supplementary Table 4 and Supplementary Fig. 24)[9,75]. Specifically, we examined how stand age directly affected local functional diversity and functional dissimilarity among local communities, and indirectly affected five temporal stability components based on our linear mixed models with the ecoregion as the random factor. We started with the conceptual model (Supplementary Fig. 24), included potential pathways if these pathways improved model fit ($P < 0.05$ for Shipley's d-separation test), and tested global model fit using Fisher's C statistic ($P > 0.05$). Standardized path coefficients were calculated for coefficient comparisons. Considering the changes in functional strategies with succession, we similarly constructed another piecewise structural equation modeling that emphasizes the effect of functional strategies on stability (Supplementary Fig. 18).

To enhance the robustness of methodology and results, we conducted the following sensitivity analysis: (1) to control the confounding effects of directional trends (reduced productivity over time due to individual aging and succession), we detrended productivity and calculated corresponding stability components. Specifically, we replaced the productivity covariance or variance as the standard deviation of the residuals of the linear regression between productivity and mean calendar year between two consecutive censuses (Supplementary Fig. 4)[21]; (2) to address this limitation of space-for-time approach, we fitted the relationship between multi-scale stability and stand age separately in each ecoregion (Supplementary Fig. 5); (3) considering the impact of time series length on temporal stability[76], we added confounding variables (survey interval, observational frequency, initial and final survey years) as fixed effects in the model 6 and evaluated the relative variable importance using '*dredge*' function in MuMIn package (Supplementary Fig. 3, Supplementary Fig. 6, and Supplementary Table S1); (4) considering the impact of long survey intervals on stability estimation, we sequentially removed plots with survey intervals larger than 5 years and fit the relationship between multi-scale stability and stand age (Supplementary Fig. 7); (5) considering changing tree diversity during the observations, we fit the stability components with the diversity in the initial year, the diversity in the middle year and the diversity in the final year (Supplementary Fig. 12); (6) considering the dependence of functional diversity on interspecific functional distance, we also calculated the functional dissimilarity among local communities considering effective species number and refitted model 6 (Supplementary Fig. 13)[77]; (7) we also added stand density and structural complexity (calculated as the coefficient of variation of individual DBH in the plot) into our analysis to control the effect of stand structure on stability (Supplementary Fig. 8); (8) considering the impact of mortality on productivity estimation, we calculate net biomass change as biomass growth of surviving trees and ingrowth by new recruitment trees minus biomass loss due to mortality, and fitted the relationship between stability of net biomass change and forest age (Supplementary Fig. 8). Meanwhile, we incorporated biomass loss due to mortality into the structural equation model to study the impact of mortality on productivity stability. (Supplementary Fig. 19); (9) we designated each plot as the focal plot, selected its three nearest plots, and treated these clustered four as a community at the larger scale[78]. Ultimately, we identified 809 communities at this scale, with a distance of 17.9 ± 7.8 km between the four plots. We then conducted a similar analysis to assess how temporal stability at the larger scale changes with stand age (Supplementary Fig. 15). These sensitivity analyzes all produced similar results to those in the main text. All statistical analyzes were performed in R (version 4.3.1).

Reporting summary

Further information on research design is available in the Nature Portfolio Reporting Summary linked to this article.

Data availability

The the USDA Forest Service Forest Inventory and Analysis Database were obtained at https://research.fs.usda.gov/products/dataandtools/tools/fia-datamart. The CRU TS climate dataset were obtained at crudata.uea.ac.uk/cru/data/hrg/. The data used in our analyzes are available at Figshare (https://doi.org/10.6084/m9.figshare.25866238). Source data are provided as a Source Data file. Source data are provided with this paper.

Code availability

R codes supporting our analyzes are available at Figshsre (https://doi.org/10.6084/m9.figshare.25866238).

References

1. Schnabel, F. et al. Species richness stabilizes productivity via asynchrony and drought-tolerance diversity in a large-scale tree biodiversity experiment. *Science Advances* **7**, eabk1643 (2021).
2. Qiao, X. et al. Latitudinal patterns of forest ecosystem stability across spatial scales as affected by biodiversity and environmental heterogeneity. *Glob. Change Biol.* **29**, 2242–2255 (2023).
3. Meng, Y., Li, S.-p, Wang, S., Meiners, S. J. & Jiang, L. Scale-dependent changes in ecosystem temporal stability over six decades of succession. *Science Advances* **9**, eadi1279 (2023).
4. Li, W. et al. Biomass temporal stability increases at two spatial scales during secondary succession. *J. Ecol.* **111**, 1575–1586 (2023).
5. Albrich, K., Rammer, W., Thom, D. & Seidl, R. Trade-offs between temporal stability and level of forest ecosystem services provisioning under climate change. *Ecol. Appl.* **28**, 1884–1896 (2018).
6. Poorter, L. et al. Successional theories. *Biological Reviews* **98**, 2049–2077 (2023).
7. Arroyo-Rodríguez, V. et al. Multiple successional pathways in human-modified tropical landscapes: new insights from forest succession, forest fragmentation and landscape ecology research. *Biological Reviews* **92**, 326–340 (2017).
8. Wang, S. & Loreau, M. Ecosystem stability in space: α, β and γ variability. *Ecol. Lett.* **17**, 891–901 (2014).
9. Wang, S. & Loreau, M. Biodiversity and ecosystem stability across scales in metacommunities. *Ecol. Lett.* **19**, 510–518 (2016).
10. Wang, S., Lamy, T., Hallett, L. M. & Loreau, M. Stability and synchrony across ecological hierarchies in heterogeneous metacommunities: linking theory to data. *Ecography* **42**, 1200–1211 (2019).
11. Li, S.-p et al. Convergence and divergence in a long-term old-field succession: the importance of spatial scale and species abundance. *Ecol. Lett.* **19**, 1101–1109 (2016).
12. Lin, S. et al. Environmental filtering drives biodiversity–spatial stability relationships in a large temperate forest region. *Funct. Ecol.* **37**, 1688–1702 (2023).
13. Staude, I. R., Weigelt, A. & Wirth, C. Biodiversity change in light of succession theory. *Oikos* **2023**, e09883 (2023).
14. Matsuo, T., Martinez-Ramos, M., Bongers, F., van der Sande, M. T. & Poorter, L. Forest structure drives changes in light heterogeneity during tropical secondary forest succession. *J. Ecol.* **109**, 2871–2884 (2021).
15. Rissanen, K., Martin-Guay, M.-O., Riopel-Bouvier, A.-S. & Paquette, A. Light interception in experimental forests affected by tree diversity and structural complexity of dominant canopy. *Agric. For. Meteorol.* **278**, 107655 (2019).

16. Bertness, M. D. & Callaway, R. Positive interactions in communities. *Trends Ecol. Evol.* **9**, 191–193 (1994).
17. Chen, H. Y. H. & Popadiouk, R. V. Dynamics of North American boreal mixedwoods. *Environ. Rev.* **10**, 137–166 (2002).
18. Hilmers, T. et al. Biodiversity along temperate forest succession. *J. Appl. Ecol.* **55**, 2756–2766 (2018).
19. Purschke, O. et al. Contrasting changes in taxonomic, phylogenetic and functional diversity during a long-term succession: insights into assembly processes. *J. Ecol.* **101**, 857–866 (2013).
20. Xu, Q. et al. Consistently positive effect of species diversity on ecosystem, but not population, temporal stability. *Ecol. Lett.* **24**, 2256–2266 (2021).
21. Tilman, D., Reich, P. B. & Knops, J. M. H. Biodiversity and ecosystem stability in a decade-long grassland experiment. *Nature* **441**, 629–632 (2006).
22. van Breugel, M. et al. Soil nutrients and dispersal limitation shape compositional variation in secondary tropical forests across multiple scales. *J. Ecol.* **107**, 566–581 (2019).
23. Taylor, A. R. & Chen, H. Y. H. Multiple successional pathways of boreal forest stands in central Canada. *Ecography* **34**, 208–219 (2011).
24. Kreyling, J., Jentsch, A. & Beierkuhnlein, C. Stochastic trajectories of succession initiated by extreme climatic events. *Ecol. Lett.* **14**, 758–764 (2011).
25. Vandermeer, J. et al. Multiple basins of attraction in a tropical forest: evidence for nonequilibrium community structure. *Ecology* **85**, 575–579 (2004).
26. Chase, J. M. Community assembly: when should history matter? *Oecologia* **136**, 489–498 (2003).
27. Qiao, X. et al. Spatial asynchrony matters more than alpha stability in stabilizing ecosystem productivity in a large temperate forest region. *Glob. Ecol. Biogeogr.* **31**, 1133–1146 (2022).
28. Wang, S. et al. Biotic homogenization destabilizes ecosystem functioning by decreasing spatial asynchrony. *Ecology* **102**, e03332 (2021).
29. Larson, A. J. & Churchill, D. Spatial patterns of overstory trees in late-successional conifer forests. *Can. J. For. Res.* **38**, 2814–2825 (2008).
30. Chin, A. R. O., Hille Ris Lambers, J. & Franklin, J. F. Context matters: natural tree mortality can lead to neighbor growth release or suppression. *For. Ecol. Manage.* **529**, 120735 (2023).
31. Hanberry, B. B. Recent shifts in shade tolerance and disturbance traits in forests of the eastern United States. *Ecological Processes* **8**, 32 (2019).
32. Hu, Y. K., Pan, X., Liu, X. Y., Fu, Z. X. & Zhang, M. Y. Above- and belowground plant functional composition show similar changes during temperate forest swamp succession. *Front Plant Sci* **12**, 658883 (2021).
33. Chazdon, R. L. et al. Composition and dynamics of functional groups of trees during tropical forest succession in Northeastern Costa Rica. *Biotropica* **42**, 31–40 (2010).
34. Sheil, D. Long-term observations of rain forest succession, tree diversity and responses to disturbance. *Plant Ecol* **155**, 183–199 (2001).
35. Schoonmaker, P. & McKee, A. Species composition and diversity during secondary succession of coniferous forests in the Western Cascade Mountains of Oregon. *For. Sci.* **34**, 960–979 (1988).
36. Connell, J. H. Diversity in tropical rain forests and coral reefs. *Science* **199**, 1302–1310 (1978).
37. Silver, E. J., Fraver, S., D'Amato, A. W., Aakala, T. & Palik, B. J. Long-term mortality rates and spatial patterns in an old-growth Pinus resinosa forest. *Can. J. For. Res.* **43**, 809–816 (2013).
38. Craven, D. et al. Multiple facets of biodiversity drive the diversity–stability relationship. *Nat. Ecol. Evol.* **2**, 1579–1587 (2018).
39. Horn, H. S. The ecology of secondary succession. *Annu. Rev. Ecol. Syst.* **5**, 25–37 (1974).
40. York, R. A., Heald, R. C., Battles, J. J. & York, J. D. Group selection management in conifer forests: relationships between opening size and tree growth. *Can. J. For. Res.* **34**, 630–641 (2004).
41. Morin, X., Fahse, L., de Mazancourt, C., Scherer-Lorenzen, M. & Bugmann, H. Temporal stability in forest productivity increases with tree diversity due to asynchrony in species dynamics. *Ecol. Lett.* **17**, 1526–1535 (2014).
42. Ledo, A. et al. Species coexistence in a mixed Mediterranean pine forest: Spatio-temporal variability in trade-offs between facilitation and competition. *For. Ecol. Manage.* **322**, 89–97 (2014).
43. Lehman, C. L. & Tilman, D. Biodiversity, stability, and productivity in competitive communities. *Am. Nat.* **156**, 534–552 (2000).
44. Yi, X. et al. From canopy complementarity to asymmetric competition: the negative relationship between structural diversity and productivity during succession. *J. Ecol.* **110**, 457–465 (2022).
45. Díaz, S. et al. The global spectrum of plant form and function. *Nature* **529**, 167–171 (2016).
46. Reich, P. B. The world-wide 'fast–slow' plant economics spectrum: a traits manifesto. *J. Ecol.* **102**, 275–301 (2014).
47. Zhang, B. et al. Species responses to changing precipitation depend on trait plasticity rather than trait means and intraspecific variation. *Funct. Ecol.* **34**, 2622–2633 (2020).
48. Chave, J. et al. Towards a worldwide wood economics spectrum. *Ecol. Lett.* **12**, 351–366 (2009).
49. West, P. W. Do increasing respiratory costs explain the decline with age of forest growth rate? *J. For. Res.* **31**, 693–712 (2020).
50. Barton, K. E. & Boege, K. Future directions in the ontogeny of plant defence: understanding the evolutionary causes and consequences. *Ecol. Lett.* **20**, 403–411 (2017).
51. Sillett, S. C. et al. How do tree structure and old age affect growth potential of California redwoods? *Ecol. Monogr.* **85**, 181–212 (2015).
52. Ryan, M. G., Phillips, N. & Bond, B. J. The hydraulic limitation hypothesis revisited. *Plant Cell and Environment* **29**, 367–381 (2006).
53. Couvreur, V. et al. Water transport through tall trees: a vertically explicit, analytical model of xylem hydraulic conductance in stems. *Plant, Cell Environ* **41**, 1821–1839 (2018).
54. Trugman, A. T. et al. Tree carbon allocation explains forest drought-kill and recovery patterns. *Ecol. Lett.* **21**, 1552–1560 (2018).
55. Wang, X. & Wang, X. Hotter drought and trade-off between fast and slow growth strategies as major drivers of tree-ring growth variability of global conifers. *J. Ecol.* **112**, https://doi.org/10.1111/1365-2745.14290 (2024).
56. Senf, C. et al. Canopy mortality has doubled in Europe's temperate forests over the last three decades. *Nat. Commun.* **9**, 4978 (2018).
57. Aakala, T., Fraver, S., Palik, B. J. & D'Amato, A. W. Spatially random mortality in old-growth red pine forests of northern Minnesota. *Can. J. For. Res.* **42**, 899–907 (2012).
58. Makoto, K. & Wilson, S. D. When and where does dispersal limitation matter in primary succession? *J. Ecol.* **107**, 559–565 (2019).
59. Liang, M. et al. Consistent stabilizing effects of plant diversity across spatial scales and climatic gradients. *Nat. Ecol. Evol.* **6**, 1669–1675 (2022).
60. Wang, S. et al. An invariability-area relationship sheds new light on the spatial scaling of ecological stability. *Nat. Commun.* **8**, 15211 (2017).
61. Walker, L. R., Wardle, D. A., Bardgett, R. D. & Clarkson, B. D. The use of chronosequences in studies of ecological succession and soil development. *J. Ecol.* **98**, 725–736 (2010).
62. Damgaard, C. A critique of the space-for-time substitution practice in community ecology. *Trends Ecol. Evol.* **34**, 416–421 (2019).
63. Patrick, C. J. et al. Multi-scale biodiversity drives temporal variability in macrosystems. *Front. Ecol. Environ.* **19**, 47–56 (2021).

64. Luyssaert, S. et al. Old-growth forests as global carbon sinks. *Nature* **455**, 213–215 (2008).
65. Watson, J. E. M. et al. The exceptional value of intact forest ecosystems. *Nat. Ecol. Evol.* **2**, 599–610 (2018).
66. Cleland, D. T. et al. *National Hierarchical Framework of Ecological Units*, (1997).
67. Woodall, C. W., Heath, L. S., Domke, G. M. & Nichols, M. C. Methods and equations for estimating aboveground volume, biomass, and carbon for trees in the U.S. forest inventory, 2010. (U.S. Department of Agriculture, Forest Service, Northern Research Station, 2011).
68. Kattge, J. et al. TRY plant trait database – enhanced coverage and open access. *Glob. Change Biol.* **26**, 119–188 (2020).
69. Jin, Y. & Qian, H. V.PhyloMaker: an R package that can generate very large phylogenies for vascular plants. *Ecography* **42**, 1353–1359 (2019).
70. Stekhoven, D. J. & Bühlmann, P. MissForest—non-parametric missing value imputation for mixed-type data. *Bioinformatics* **28**, 112–118 (2011).
71. Laliberté, E. & Legendre, P. A distance-based framework for measuring functional diversity from multiple traits. *Ecology* **91**, 299–305 (2010).
72. Harris, I., Osborn, T. J., Jones, P. & Lister, D. Version 4 of the CRU TS monthly high-resolution gridded multivariate climate dataset. *Sci. Data* **7**, 109 (2020).
73. Poggio, L. et al. SoilGrids 2.0: producing soil information for the globe with quantified spatial uncertainty. *Soil* **7**, 217–240 (2021).
74. Bates, D., Maechler, M., Bolker, B. M. & Walker, S. C. Fitting linear mixed-effects models using lme4. *J. Stat. Softw.* **67**, 1–48 (2015).
75. Lefcheck, J. S. piecewiseSEM: Piecewise structural equation modelling in r for ecology, evolution, and systematics. *Methods Ecol. Evol.* **7**, 573–579 (2016).
76. Luo, M. et al. The effects of dispersal on spatial synchrony in metapopulations differ by timescale. *Oikos* **130**, 1762–1772 (2021).
77. Chao, A. et al. An attribute-diversity approach to functional diversity, functional beta diversity, and related (dis)similarity measures. *Ecol. Monogr.* **89**, e01343 (2019).
78. Li, J. et al. Tree diversity across multiple scales and environmental heterogeneity promote ecosystem multifunctionality in a large temperate forest region. *Glob. Ecol. Biogeogr.* **33**, e13880 (2024).

Acknowledgements

We thank hundreds of FIA field crew members for the data used in our study. This research was supported by Shenzhen Science and Technology Program (JCYJ20230807111116034 for Z.M.), Guangdong Basic and Applied Basic Research Foundation (2023A1515010643 for Z.M.), National Natural Science Foundation of China (32101272 for Z.M.) and Fundamental Research Funds for the Central Universities, Sun Yat-sen University (23lgbj009 for Z.M.). We thank Eric Searle for providing proofreading assistance during the revision. We thank Prof. Shaopeng Wang, Lin Jiang, and Shaopeng Li for providing theoretical assistance during the study. We thank the tree image in Fig. 1 designed by macrovector - Freepik.com.

Author contributions

R.S. formulated the research question. R.S., G.F., and Y.L. extracted the data and performed the analysis. R.S. wrote the first draft of the manuscript with assistance from G.F., Y.L. and Z.M.. R.S. and Z.M. contributed substantially to the manuscript revision. Z.M. supervised the project and provided essential suggestions and funding support.

Competing interests

The authors declare no competing interests.

Additional information

Supplementary information The online version contains supplementary material available at https://doi.org/10.1038/s41467-025-57984-3.

Correspondence and requests for materials should be addressed to Zilong Ma.

Peer review information *Nature Communications* thanks Rodrigo Muñoz, and the other, anonymous, reviewers for their contribution to the peer review of this work. A peer review file is available.